Journal of Manufacturing Engineering, 2007, Vol.2, Issue.2

UNCERTAINTY QUANTIFICATION BASED MULTI-OBJECTIVE OPTIMIZATION FOR ENGINEERING SYSTEMS

Kaushik Sinha

DaimlerChrysler Research and Technology, Bangalore –560001, India

E-mail: Kaushik.Sinha@daimlerchrysler.com

ABSTRACT

This paper presents a methodology for uncertainty quantification based multi-objective optimization of automotive body components under impact scenario. Conflicting design requirements arise as one tries, for example, to minimize structural mass while maximizing energy absorption of an automotive rail section under structural and occupant safety related performance measure constraints. Uncertainty quantification is performed in broadly using two methods: reliability based approach and robustness based approach. Deterministic, reliability-based and robustness based multi-objective optimization solutions are compared. A genetic algorithm based multi-objective optimization software reliaGDOT, developed in-house, is used to come-up with an optimal pareto-front in all cases. The technique employed here treats multiple objective functions separately without combining them in any form. A decision-making criterion is subsequently invoked to select the "best" subset of solutions from the obtained non-dominated Pareto optimal solutions. The pareto optimal set obtained in case are compared and contrasted and observations made comparing reliability based approach *vis-à-vis* robustness based approach. Looking at a broader picture, this methodology can potentially fill the gap between numerically optimized system development and simulation-driven digital product development. This, in turn, help realize numerical simulation-driven product development process by aiming to achieve designs that are "first time right". In addition, this approach can be used as a part of a target cascading technique, integrating organization wide product development process using appropriate methods (e.g., design structure matrix).

Keywords: *Uncertainty Quantification*, *Energy Absorption*, *reliaqDOT*, *Pareto Optimal Solutions*

1. INTRODUCTION

The highly competitive nature of the automotive industry demands continuous product innovation and reduction in product development cycle time while satisfying ever-increasing performance and regulatory requirements. Numerical design optimization, embedded in a simulation-driven product development framework, provides a scientific approach to automatically determine the most efficient designs under the target operating environment. When a multidisciplinary design optimization method is used, the deterministic optimum design is frequently pushed to the design constraint boundary, leaving very little or no room for tolerances (or uncertainties) in design, manufacturing, and operating processes. Consequently, deterministic optimum design that is obtained without consideration of such uncertainties can result in unreliable design, underscoring the need for reliability-based design optimization (RBDO). The basic difference between deterministic and reliability/robustness based approach is that we get optimal" design solution with the first variant, while optimal "mean" design points are derived from second variant. Crash simulation gives crash-based safety design engineers the opportunity to explore many more alternative designs than they could with hardware. A feasibility study of vehicle safety CAE optimization single objective) has been done [1]. Approximate methods for safety optimization of large systems were compared in terms of accuracy and effectiveness [2]. RBDO for vehicle crashworthiness was attempted using the Monte Carlo Simulation (MCS) method on a global response surface [3]. But all these studies were done for single objective and multiple constraints. In such a case, there is a single optimal design point assuming optimal solution exists). In case of multiple, conflicting objectives driving a design under a set of constraints, there would be no single optimal design point, but a set of "optimal" points in the objective space. The set is referred to as pareto optimal front. To the best of author's knowledge, reliability based multi-objective optimization of automotive components has not been reported in the literature. The same is true for robust multi-objective optimization formulation. Since crash

analysis is computationally intensive, a global response surface, generated with the optimal LHS Design of Experiment (DoE) [4], is treated as the original problem for RBDO. The rationale for this approach is that the global response surface may have the characteristic of the design dependency and the main purpose is to show the proposed RBDO methodology for a large-scale problem. Two different approaches have been used for reliability computation in this work: mean value approach or the approximate moment approach (AMA) and reliability index approach (RIA). Robustness has been introduced using mean-value based approach.

2. DETERMINISTIC MULTI-OBJECTIVE FORMULATION

A deterministic multi-objective optimization problem with (M) objective and (P) constraints is stated as below:

Minimize f(X) = (f1(X),f2(X),…,fM(X))
Subject to:

$G_1(X) \leq 0$
$G_2(X) \leq 0$
.
.
$Gp(X) \leq 0$

Here the objective is a " vector" with M-components and therefore is also termed as " vector" optimization problem. Here, the objective functions lie in a multidimensional space, in addition to the usual multidimensional design variable space. For each solution X in the design variable space, there exists a point in the objective space Z = [f_1(X), f_2(X), …., f_M(X)]. The output is not a single point, but a set of non-dominated points designated as pareto optimal set, which conforms to a partial order relation. A pareto optimal solution that is better with respect to one objective requires a compromise in at least one other objective.

3. RELIABILITY BASED MULTI-OBJECTIVE OPTIMIZATION FORMULATION

In system parameter design, the reliability-based multi objective design optimization (RBMODO) problem can be stated as:

Minimize f(X) = (f_1(X),f_2(X),…,f_M(X))
Subject to:

$$P(G_i(X) \geq 0) \leq \Phi(-\beta_{ti})$$

Where $i=1...,p$

β_{ti} represents the cumulative distribution function of standard normal distribution with β_{ti} being the prescribed reliability target corresponding to i-th constraint. The constraints can also be cast in another format relating safety reliability index β_{si} to prescribed reliability target such that $\beta_{si} \geq \beta_{ti}$ this formulation is used for all reliability constraint formulations in this work. One striking difference between the deterministic and reliability based optimization is that, in the reliability based optimization, the optimized parameters are the "mean" optimal values rather than "the" optimal values. This is because, reliability based optimization formulation assumes variation about "mean" values and makes sure that the optimal design thus arrived do not fail in any performance criteria (e.g., constraints) due to these variations (see figure. 1). In reliability based optimization approaches, the additional computation step is computation of safety reliability index β_{si}. Two approaches have been tried for computation of β_{si}.

3. APPROXIMATE MOMENT APPROACH (AMA)

AMA does not require information about the probability distribution of design variables, but require derivative information of performance constraints with respect to design variables about their mean values. The performance function G(X) is expanded at the mean value point using Taylor series:

$$G(X) \cong G(\mu) \sum_{i=1}^{n} \frac{\partial G(\mu)}{\partial X_i}(X_i - \mu_i) \qquad \text{-(1)}$$

The variance is approximated as:

$$\sigma_G^2 = \int_{-\infty}^{\infty} [G(X) - G(\mu)]^2 dX$$

$$\cong \sum_{i=1}^{n} \left[\frac{\partial G(\mu)}{\partial X_i} \right]^2 \int_{-\infty}^{\infty} (X_i) - G(\mu_i)^2 dX$$

$$= \sum_{i=1}^{n} \left[\frac{\partial G(\mu)}{\partial X_i} \sigma_{xi} \right]^2 \qquad (2)$$

The safety reliability index is computed as:

$$\beta_{si} = \frac{G(\mu)}{\sigma_G} \qquad (3)$$

This is the simplest possible approach and no detailed probabilistic distribution models are required. But this approximation may yield inaccurate results if ***X***

is not close to the mean value $\boldsymbol{\mu}$, which occurs if the standard deviation of the random variable $\boldsymbol{X}$ is large [6].

4. FIRST-ORDER RELIABILITY INDEX APPROACH (RIA)

This is a detailed probabilistic analysis based evaluation approach. In this case, the analysis is performed in two different random spaces: the original random design variable space (X-space) for design optimization and the independent standard normal space (U-space) for reliability analysis [5, 6]. During the reliability based multi-objective optimization process, a transformation between X and U space at design points must be carried out for estimating the probabilistic constraints. The transformation between two different random spaces at the design point d^k is defined as:

$$U=T(X) \text{ where } d^k = \mu^k(X) \qquad (4)$$

It is assumed that, no correlation exists among the design variables. This requires probability distribution information for each input random variable. Most of the transformations from X to U-space are nonlinear, except in case of normal distribution. In RIA, the first-order safety reliability index is obtained by formulating an optimization problem with an equality constraint in U-space, which is the failure surface, as

$$\begin{aligned} &\text{minimize} \quad \|U\| \\ &\text{subject to } G(U) = 0 \text{ --} \end{aligned} \qquad (5)$$

The minimum point on the failure surface is called the

Most Probable Point (MPP) $u^*_{G(u)} = 0$ and the safety reliability index is defined by $\beta_{si} = \| u^*G(u)=0\|$. To find the solution to either an MPP search algorithm that has been specifically developed for the first-order reliability analysis or a general optimization algorithm can be used. Due to its simplicity and efficiency, the HL-RF method is a popular choice for conducting a reliability analysis in RIA, and the same has been used in this work. The iterative algorithm of the HL-RF method is,

$$u^{(k+1)} = (u^{(k)}.n^{(k)})n^{(k)} + \frac{\nabla G(u^{(k)})}{\| \nabla G(u^{(k)}) \|} n^{(k)} \qquad (6)$$

Where

$$n^{(k)} = -\frac{\nabla G(u^{(k)})}{\| \nabla G(u^{(k)}) \|}$$

is the steepest descent direction of the performance function G_u at $\boldsymbol{\mu}^k$. The first term on the right side of the iterative relation above finds a direction with the shortest distance to the failure surface, and the second term is a correction term to reach G (U). Post optimization, the probability of failure (P_f) is computed using the following formulae:

$$P_f = \Phi(-\beta) = \frac{1}{2}[1 + erf(-\beta/\sqrt{2})] \text{ for } \beta \le 8.0$$

$$= \frac{1}{\beta\sqrt{2\pi}} e^{-\frac{\beta^2}{2}} \text{ for } \beta > 8.0$$

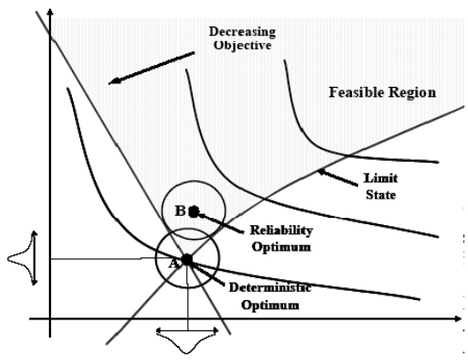

Figure 1 - Geometric interpretation of deterministic and reliability-based design optimal solutions.

5. ROBUSTNESS BASED MULTI-OBJECTIVE OPTIMIZATION FORMULATION

In multi-objective robust design approach, the mean values of the objective functions are optimized while the coefficient of variation (CoV), which is the ratio between standard distribution and mean value, for each objective function is set to a small permissible value. This ensures insensitivity of objectives to uncertainty. In this approach, each constraint is formulated taking into account the standard deviation, mean value and target robustness level. The robustness (one-sided) based multi-objective optimization problem is stated as:

Minimize $f(X) = (f_1(X), f_2(X), \ldots, f_M(X))$
Subject to:

$$G_i(\mu) + k_i \sigma_{G_i} \le 0 \text{ where, } i = 1,.., p$$

$$CoV_j^2 = \left(\frac{\sigma_{f_i}}{\mu_{f_j}}\right)^2 \le CoV_{tj}^2$$

where j=1,..,M

The second set of constraints on the variation of is built at the runtime as a set of internal constraints. For each physical constraint, (k_i) denotes the desired sigma quality level. For example, k_i = 6.0 denotes six sigma quality/robustness level. In this case as well, the optimal pareto front is actually the "mean" optimal pareto front. Robustness criteria typically shifts the optimal design

points from a probable " ridge" to a relative " valley" (refer to figure. 2) where design solutions are less affected by parameter variations (robust design points).

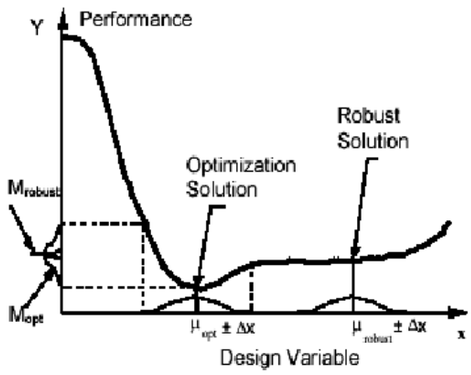

Figure 2 - Difference between robust solution and "optimal" solution.

Usually (although not necessarily) robust solution is suboptimal to corresponding reliable solution, which is, in turn, suboptimal to deterministic optimal.

6. MULTI-OBJECTIVE OPTIMIZATION APPROACH

A multi-objective optimization problem (MOOP) involves a number of objective functions to be optimized simultaneously. One of the striking differences between single and multi-objective optimization is that in MOOP, the objective functions lie in a multi-dimensional space, in addition to the usual multi-dimensional design variable space. For each solution X in the design variable space, there exists a point in the objective space $Z = [f_1(X), f_2(X), \ldots, f_m(x)]$.

Mathematically this becomes a partial order and we require some higher-level information to transform this into a total order to enable comparison operations [8,9]. The output of a MOOP is not a single point, but a set of non-dominated points designated as pareto optimal set, which conforms to a partial order relation. A pareto optimal solution that is better with respect to one objective requires a compromise in at least one other objective [9]. There are two principal goals of multi-objective optimization:

1. Find a set of solutions close to the pareto optimal solutions, and
2. Find a set of solutions, which are diverse enough to represent the entire spread of the pareto optimal front.

After a set of non-dominated optimal solutions in objective space is found, user can then use higher-level qualitative information to make specific choices. For an ideal multi-objective optimization procedure, there are two steps [10]:

1. Find a diverse pareto optimal set of non-dominated solutions.
2. Choose one of the candidate optimal solutions based on higher-level information.

ReliaGDOT internally uses the NSGA-II algorithm [10, 11] for finding pareto optimal set has three basic features:

1. It uses elitist principle for population generation.
2. It uses an explicit diversity preserving mechanism, and
3. It emphasizes non-dominated solutions in a population.

There are two basic definitions used to enforce domination of one solution over the other:

Definition 1 *A solution x(i) is said to dominate the other solution x(j), if both the following conditions are true:*

1. *The solution x(i) is no worse than x(j) all objectives.*
2. *The solution x(i) is strictly better than x(j) in at least one objective.*

In presence of constraints, each solution can be either feasible or infeasible. The constrain-domination condition for any two solutions is defined as:

Definition 2 *A solution x(i) is said to 'constrain dominate' a solution x(j), if any of the following conditions are true:*

1. *Solution x(i) is feasible and x(j) is not.*
2. *Solutions x(i) and x(j) are both infeasible, but solution x(i) has a smaller constraint violation.*
3. *Both solutions are feasible and solution x(i) dominates solution x(j) in the usual sense of definition 1 above.*

One has to select one pareto optimal point instead of many and this requires a higher level, user-specified information. Mathematically, this operation converts a partial order relation (pareto optimal set) to a total order relation to enable comparison. Most of the time, the chosen point belongs to a region in the pareto optimal front that 'bulges' out the most and lie somewhat 'in the middle' of the front. This point is termed as the '*knee point*'. It is characterized by a point that lies farthest from the surface connecting each individual optimal point for each objective (refer to figure. 3). A point given by the optimal values of each individual objective is termed as the '*utopia point*'. This

point cannot be attained in practice in the presence of conflicting objectives.

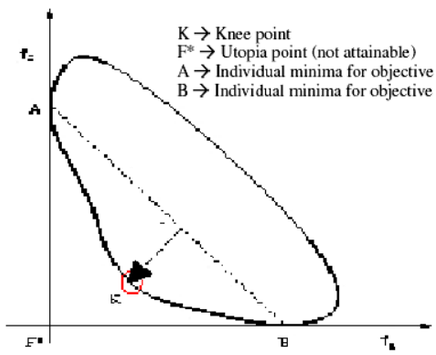

Figure 3 - The point (K) on the pareto-front having largest distance from line AB, connecting individual minima, is termed *knee point*

7. NUMERICAL EXAMPLES

7.1 Problem definition

Two examples are considered in this study: (i) crashworthiness of an automotive rail section; (ii) automotive bumper system design for low velocity frontal impact. Automotive rail sections are supposed to absorb the most of impact energy in case of a frontal crash, while bumpers systems are designed to absorb a sizeable share of the impact energy in case of a low velocity impact and insulating other structural components from damage.

1 Automotive rail section design

This study considers a box-shaped, energy-absorbing front-end rail structure (refer figure. 4). Crashworthiness is studied by crashing the rail-section into a rigid wall with a collision velocity of 6.67 m/sec. The rail section is fixed at the base and 4-noded linear elements are used with spot-welds connecting the top and bottom sections (refer figure. 4). The finite element models developed is solved using LS-DYNA. Failure plastic strain is specified in the material model for all models, but no strain-rate sensitivity is considered. The design variables considered are top and bottom thickness (t_1 and t_2) and material yield strength (σ_y). There is another linked design parameter in material young's modulus (E). Thickness parameters are considered continuous while the material yield strength can attain a discrete set of values. The material young' s modulus is related to its yield strength using the following relation:

$$E = E_0 + \Delta * (\sigma_y - \sigma_{y,l})/(\sigma_{y,u} - \sigma_{y,l}) \quad \ldots\ldots (7)$$

Where,
E_0 = base value of young's modulus (190 GPa in this study)
Δ = Range of permitted young's modulus (30 GPa in this study)
σ_y = Yield strength of the material in GPa
$\sigma_{y,u}$ = Upper value of yield strength (0.7 GPa in this study)
$\sigma_{y,l}$ = Lower value of yield strength (0.2 GPa in this study)

This linking relation ensures that young's modulus can take only discrete values. The responses considered for meta model development are structural weight, maximum transmitted force (using SAE 1000 filter), maximum intrusion, internal energy, crash pulse efficiency and energy absorption efficiency. The pulse efficiency and energy absorption efficiency are derived measures (composite function involving two primary responses) and computed as:
Pulse efficiency (%),
P =100*(Area under force-displacement curve / F_{max}*D_{max})
where, F_{max} = maximum transmitted force
D_{max} = maximum intrusion
Design exploration is performed using Latin hypercube technique for selection of design points where numerical experiments are performed using finite element models. In this study, structural weight and energy absorption efficiency are treated as objectives with pulse efficiency as a constraint, in addition to constraints on maximum force, intrusion.

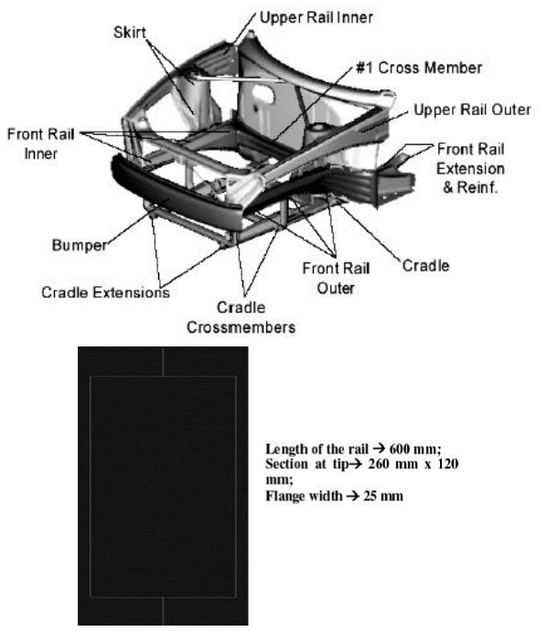

Figure 4 - Representative front end (ULSAB) and Rail section

Response surface models up to 2-nd order (quadratic) are considered in this study. This approximate model is defined only within the specified design space. In all, 32 points are generated using Latin Hypercube technique with three design variables for conducting "numerical experiments". The Latin Hypercube technique is chosen because it covers the whole design space and is reported to have performed better than other techniques while modeling highly non-linear responses [7]. The permissible values of material yield strength variable are {0.20, 0.30, 0.35, 0.40, 0.45, 0.50, 0.55, 0.60, 0.65, 0.70}.

2. Bumper system design

The allowable intrusion is an important factor in the design of bumper systems. Smaller offsets between the bumper face and the first damageable vehicle component require new ideas for absorbing the energy of low-speed impacts with lower intrusion, while limiting the transmitted rail loads. Bumper designs must therefore satisfy two distinct and conflicting requirements:

- Maximize energy absorption for a given packaging space.
- Minimize maximum intrusion while limiting the transmitted rail loading.

In low-speed impacts, the kinetic energy of the vehicle converted into work done on the bumper system. The overall energy to be dissipated during a rigid barrier impact is given by:

$$E_d = \tfrac{1}{2}MV^2 \text{ ------- (8)}$$

Where M = vehicle mass (kg); V = closing speed of vehicle (m/sec).

Typically, a small amount of impact energy is absorbed by the attached vehicle components due to vibrations and vehicle compliance. Therefore, the actual energy required to be absorbed by the bumper is slightly less than the total dissipation energy given in Eq.8 and is represented by a factor η. Typical values for η for a barrier impact ranges from 0.82-0.90 [7]. The value taken for this study is 0.90. The energy to be dissipated by the bumper system is therefore given by: The value taken for this study is 0.90. The energy to be dissipated by the bumper system is therefore given by:

$$E_{bumper} = \tfrac{1}{2}\eta MV^2 \text{ ------ (9)}$$

The bumper system manages this energy by moving a force **F** (resistance to deformation) through a distance **d** (intrusion).The work done is given by the area under the force displacement curve (figure 5).

$$E_{bumper} = Fd \text{ ------ (10)}$$

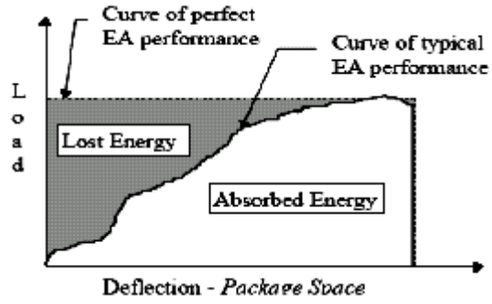

Figure 5 - Ideal vs. Typical energy absorption model

Since the bumper is not 100% efficient (see figure. 2), an efficiency factor (ε) is included:

$$E_{bumper} = \varepsilon Fd \text{ ------ (11)}$$

This factor takes care of the situation where rail loading does not build-up immediately (which is the ideal situation resulting in square waveform). Force is related to deceleration of bumper system (a) as:

$$F=Ma \qquad (12)$$

Inserting Eq.(12) into Eq.(11) yields,

$$E_{bumper} = \varepsilon Mad \text{ ------ (13)}$$

Equating Eq. 9 and Eq. 13 provide the energy absorption efficiency:

$$\varepsilon = \frac{\eta V^2}{2ad} \text{ -------- (14)}$$

The ideal scenario for energy absorption is a square shaped force-displacement curve. But this requires instantaneous build-up for force and sustenance of the same over the complete crash event, which is not achievable at present. As an automobile collides with another object, both the occupant and the vehicle can undergo rapid changes in acceleration/deceleration profile. Increasing the level of energy absorption in the front end of the vehicle can significantly lower the vehicle' s peak deceleration, resulting in lower occupant velocities relative to vehicle interior. Hence, greater the energy absorption, the lower the occupant velocity and less severe is the impact to the occupant in the passenger compartment. In this study, the responses considered are as follows:

- Energy absorption efficiency (%).
- Barrier intrusion.
- Maximum force transferred to bumper system.
- Maximum plastic strain (both EA and backup beam).

The design space, in terms of 6 design variables, is given illustrated in the table below:

Table 1 - Design space definition for bumper system

Design variable (mm)	Lower limit	Upper limit
Outer Radii	1374	3075
Inner Radii	1420	4111
Centre depth	50	95
EA thickness	1.5	2.5
Rail span	1010	1483
Backup beam thickness	1.26	1.56

Design of Experiments (DoE) was performed with 30 experimental points using the Latin Hypercube strategy. The statistical parameters checked for transfer function quality are R^2, R^2 adjusted for each model and also p-values for each term included in a model. These transfer functions are used in all optimization studies and the optimized solution is validated using LS-DYNA.

7.1.1 Automotive rail section design optimization

Here the structural weight (W) is minimized along with maximization of energy absorption efficiency (E). The constraints are on maximum transmitted force (F_{max}) and maximum intrusion (D_{max}) and crash pulse efficiency (P). The problem is formulated as follows:

Minimize Structural weight (W)

Maximize energy absorption efficiency (E) … (15)

Such that,

$F_{max} \leq 200.0$ kN
$D_{max} \leq 190.0$ mm
$P \geq 18$ %
$0.50 \leq t1,\ t2 \leq 2.0$
σ_y -> {0.20, 0.30, 0.35, 0.40, 0.45, 0.50, 0.55, 0.60, 0.65, 0.70}

In case of reliability based optimization, all the design variables are assumed to be normally distributed with coefficient of variation of 0.05 (5%). The target reliability indices (β_{ti}) for first two constraints are set to 6.0 while the third constraint has a beta target value of 3. The reliability based multi-objective design optimization (RBMODO) statement becomes:

Minimize Structural weight (W)
Maximize Energy absorption efficiency (E) …(15B)

Such that

$G_1(\mu) + 6\sigma_{G1} \leq 200$ (Constraint on max. Force)

$G_2(\mu) + 6\sigma_{G2_t} \leq 190$ (Constraint on max. Intrusion)

$G_3(\mu) + 3\sigma_{G3_t} \geq 18$ (Constraint on pulse efficiency (%))

$$CoV_j^2 = \left(\frac{\sigma_w}{\mu_w}\right)^2 \leq 0.0016$$

$$CoV_j^2 = \left(\frac{\sigma_E}{\mu_E}\right)^2 \leq 0.0036$$

$0.50 \leq t_1, t_2 \leq 2.0$

$0.20 \leq \sigma_y \leq 0.70$

Bumper system design optimization

The bumper system multi-objective design optimization problem is formulated as:

Maximize Energy absorption efficiency = f1 (X)
Minimize Barrier intrusion = f 2(X)---- (16)

Subject to:

Maximum transmitted force ≤ F limit
Maximum plastic strain in EA ≤1.2
Maximum plastic strain in beam ≤0.25

In this study, limit of 100kN was set for maximum transmitted force. In case of reliability based optimization, all the design variables are assumed to be normally distributed with coefficient of variation of 0.05 (5%). The reliability based multi-objective design optimization (RBMODO) statement becomes:

Maximize Energy absorption efficiency = f1 (X)
Minimize Barrier intrusion = f 2(X) --- (16A)

Subject to:
$\beta t1 \geq 0.6$ Constraint on max. Force
$\beta t2 \geq 0.6$ -- Constraint on max. plastic strain in EA
$\beta t3 \geq 0.6$ -- Constraint on max. plastic strain in beam

The corresponding robustness based multi-objective design optimization problem with all the design variables are assumed to be normally distributed with coefficient of variation of 0.05 is stated as:

Maximize Energy absorption efficiency = f1 (X)
Minimize Barrier intrusion = f 2(X) ---- (16B)

Subject to

$G_1(\mu) + 6\sigma_{G1} \leq 110$ (Constraint on maximum Force)

$G_2(\mu) + 6\sigma_{G2_t} \leq 1.2$ (Constraint on maximum plastic strain in EA)

$G_3(\mu) + 6\sigma_{G3_t} \leq 0.25$ (Constraint on max. plastic strain in beam)

$$CoV_j^2 = \left(\frac{\sigma_{f_1}}{\mu_{f_1}}\right)^2 \leq 0.0025$$

$$CoV_j^2 = \left(\frac{\sigma_{f_2}}{\mu_{f_1}}\right)^2 \leq 0.0025$$

8. RESULTS & DISCUSSION

8.1 Automotive rail section design optimization results

The results of deterministic multi-objective optimization are summarized below:

Table 2 a & b - Summary of results for deterministic multi-objective optimization

Pareto point	t_1	t_2	$\tilde{y}$	Knee Weight	E (%)
Knee point	1.185	0.505	0.70	3.6792 *(3.679)	74.61 (74.98)
Minima W	0.95	0.52	0.70	3.19	58.61
Maxima W	1.42	0.5	0.70	4.165	87.33

*Quantities in brackets indicate analysis results obtained from LS- DYNA simulation.

Pareto point	F_{max}	D_{max}	P (%)
Knee point	162.37 (161.2)	166.7 (164.82)	19.26 (19.32)
Minima W	126.36	179.8	**18.08**
Maxima E	**197.82**	156.33	19.92

As can be seen, the crash pulse efficiency is relatively close to the constraint boundary in majority of the cases. At knee point, the design is not very close to any constraint boundary. Maximum force constraint is active when maximizing for energy absorption only. This design indicates higher structural weight, but crash pulse efficiency is also improved. Another interesting observation is that, different thickness for the two panels with higher yield strength steel (AHSS) is advocated for optimal performance. Higher yield strength seems better from energy absorption view point. While using reliability based optimization, the "optimal" pareto front shifts from that of deterministic version and depends on the target reliability indices used. In addition "optimal" pareto solution sets obtained using two different variants of safety reliability index computation method are plotted in the figure. 6 below. Here, the pareto optimal solutions corresponding to the knee point solution is taken for both RIA based and AMA based solution and reliability is computed for each constraint using MCS. In all cases 10000 samples were used and RMCS > 0.999 were obtained for all cases. It is observed from the results that the reliability based pareto optimal fronts and also the robust pareto optimal front have shifted below the corresponding deterministic pareto optimal front. This result is along expected lines, but another observation is that of a 'jump' in the pareto optimal front. The same problem was run with increased number of generations (200 and 400 generations) to check if it has really converged and make sure that such behaviour is not due to algorithmic issues. This discontinuity is observed in terms of energy absorption efficiency. For two pareto optimal points with very close structural weight gives a very different energy absorption efficiency (marked as '*knee point*' and '*significant point*' in table 3a-b). This 'jump' seem to be controlled by the constraint activity and material yield stress property (material yield stress does not appear in structural weight calculation so long as unit weight remains the same). Higher yield AHSS gives better energy absorption while satisfying all reliability constraints with pulse efficiency being very close to constraint boundary.

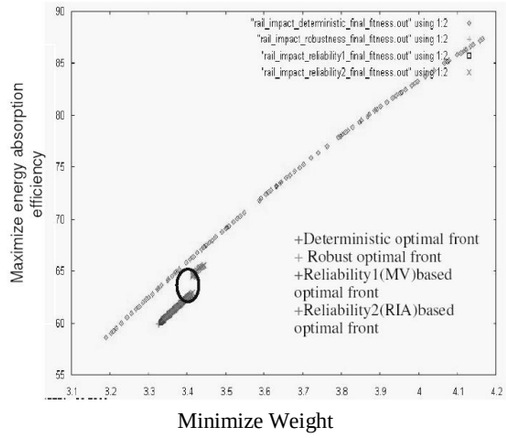

Figure 6 - Pareto optimal front obtained using different approaches

It is also observed that the '*span*' of the reliability based or robustness-based pareto optimal fronts are much

smaller as compared to the deterministic front in this case.

Table 3 a & b - Summary of results for reliability-based multi-objective optimization using RIA

Pareto point	t_1	t_2	$\tilde{y}$	Knee Weight	E (%)
Knee point	1.012	0.545	0.65	**3.4142** *(3.414)	**64.46** (64.58)
Minima W	0.021	0.5	0.60	3.3387	60.364
Maxima W	1.052	0.52	0.65	3.4435	65.558
Significant point	1.056	0.501	0.60	**3.41418**	**62.932**

*Quantities in brackets indicate analysis results obtained from LS-DYNA simulation.

Pareto point	β_1	β_2	β_3
Knee point	**6.543**	**7.212**	3.001
Minima W	6.848	6.048	3.344
Maxima W	6.028	**7.432**	3.11
Significant point	**6.021**	**6.40**	3.775

Such 'jump' or discontinuity can also indicate possible system instability in certain cases (e.g., dynamical systems). In this case, the robust pareto front almost coincides with the reliable pareto front.

8.2 Bumper system design: results

As the *maximum transmitted force limit is increased*, *the barrier intrusion reduces* and also the *efficiency of the bumper increase*. This situation is advantageous in both objectives. A higher value of limiting maximum transmitted force leads to better pulse (closer to a square pulse) and there is a threshold value of this quantity from the structural behaviour standpoint. The centre depth are at its upper limit of 95 mm. EA thickness is on the higher side (approaching upper limit) for all points on the pareto front. The back-up beam thickness bar chart indicates no extreme behaviour in terns of reaching the limit values. The constraint on maximum transmitted rail loading is active (e.g., close to the constraint boundary). The results of multi-objective optimization for two cases considered are summarized below:

Table 4 - Summary of results for deterministic multi-objective optimization for case 1 (limiting force = 100kN)

Pareto point	intrusion (I) (mm)	Energy absorption efficiency (ε) (%)	Transmitted rail load(F) (kN)
Knee point	[1]91.00 (89.9)	62.077 (63.48)	99.97 (99.9)
Minima I	88.535	59.92	99.98
Maxima	96.8	62.7	99.92

ε

In this problem, the '*span*' of the reliability-based and robustness-based pareto optimal fronts are much wider as compared to the deterministic front. The optimal front still shifts below their deterministic counterpart as expected.

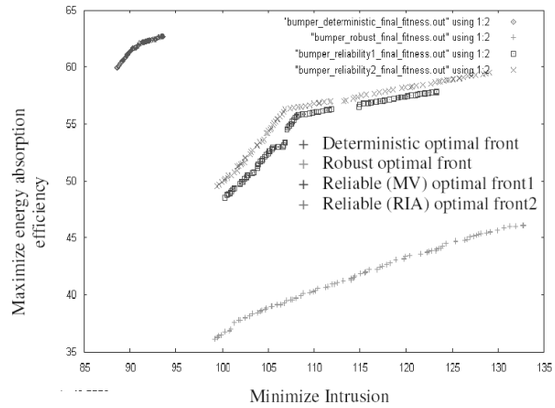

Figure 7 - Pareto optimal front with 100 kN rail loading constraint on bumper for different approaches

Here, the pareto optimal solution corresponding to the knee point solution is taken for both RIA based and AMA based solution as before and reliability is computed for each constraint using MCS. In all cases 10000 samples were used. The computed reliability, RMCS > 0.9992 were observed for solution obtained using RIA for reliability index computation. In case of AMA, RMCS > 0.9989 were observed for the constraint. In this problem, the robust pareto front is more conservative than the reliable pareto front as expected.

9. CONCLUSIONS

This study illustrates use of an integrated probabilistic design optimization framework capable of supporting multi-disciplinary, multi-objective optimization process. This theme is central to any simulation based design synthesis approach. Different uncertainty (only aleatory uncertainty is considered in this study) quantification techniques have been studied in the context of multi-objective optimization. The basic multi-objective optimization is performed using the GDOT software, developed by the author's. When uncertainty is taken into consideration, the "optimal" pareto front shifts towards a "safer" region where parameter uncertainties no longer impact the feasibility of the optimal design solutions. As a preliminary observation, it can be seen that robustness based optimal" front is more " conservative" , that is, it is further away from the

deterministic " optimal" front as compared to the reliability-based optimal front. This also corroborates the view that the robust front is suboptimal to the reliable front. But this is still initial days and more numerical investigation for varying categories of problems are required before we can make a "strong" claim. In addition, in reliability based approaches, AMA looks more conservative in terms of computing the safety reliability index as compared to RIA approach. But this could only be valid if all uncertainties are modeled using normal distribution. One needs to test different types of probability distributions for modeling design parameters to put forth a claim in this regard. In future, performance measure approach (PMA) needs to be implemented for formulating the probabilistic constraints as another reliability based approach. The accuracy of adopted global response surface for probabilistic constraint modeling also should be investigated in detail. Looking at a broader picture, this methodology can potentially fill the gap between numerically optimized system development and simulation-driven digital product development. This, in turn, help realize numerical simulation-driven product development process by aiming to achieve designs that are "first time right".

10. REFERENCES

1. Yang, R.J.; Tseng, L.; Nagy, L.; Cheng, J. 1994, *"Feasibility study of crash optimization"*. ASME 69(2), 549–556.
2. Yang, R.J.; Gu, L.; Liaw, L.; Gearhart, C; Tho, C.H.2000, *"Approximations for safety optimization of large Systems"*. 26th ASME Design Automation Conference, DETC2000/DAC- 14245, Baltimore, MD
3. Gu, L.; Yang, R.J.; Cho, C.H.; Makowski, M.; Faruque, M.; Li, Y. 2001, *"Optimization and robustness for crashworthiness"*. Int. J. Vehicle Des. 26(4)
4. Currin, C.; Mitchell, T.; Morris, M.; Ylvisaker, D. 1991, *"Bayesian prediction of deterministic function with applications to the design and analysis of computer experiments"*. J. Am. Stat. Assoc. 86, 953–963.
5. Liu, P.L, and Kiureghian, A. D., 1991, *"OptimizationAlgorithms for Structural Reliability"*, Struct. Safety, 9, pp. 161-177.
6. Youn, B.D., Choi, K.K, 2004, *"Selecting Probabilistic Approaches for Reliability-based design optimization"*, AIAA, Vol. 42, No. 1.
7. Darin Evans, *"Consistency of Thermoplastic Bumperbeam Impact Performance"*, SAE Paper No. 980113.
8. Kreyszig, Erwin 1989: *"Introductory functional analysis with applications"*, Wiley Classics Library.
9. Miettinen, K. 1999, '*Nonlinear Multiobjective Optimization'*, Kluwer Academic Publishers, Boston.
10 K, Deb 2001, *" Multi-objective optimization using evolutionary algorithms*". Chichester, UK: Wiley.
11. K. Deb; S. Agrawal; A. Pratap; and T. Meyarivan, *"A fast and elitist multi-objective genetic algorithm: NSGAII"*.IEEE Transactions on Evolutionary Computation, 6(2): 182–197, 2002.